

Supplementary Information

Systems-level chromosomal parameters represent a suprachromosomal basis for the non-random chromosomal arrangement in human interphase nuclei

Sarosh N. Fatakia^{1*}, Ishita S. Mehta^{1,2} and Basuthkar J. Rao^{1*}

¹Department of Biological Sciences, Tata Institute of Fundamental Research, Mumbai,
Maharashtra 400005, India.

²UM-DAE Centre for Excellence in Basic Sciences, Biological Sciences, Kalina campus,
Santacruz (E), Mumbai, Maharashtra 400098, India.

* Corresponding authors: Dr. Sarosh N. Fatakia, Email: sarosh.fatakia@tifr.res.in
and Professor Basuthkar J. Rao, Email: bjrao@tifr.res.in

Phone number: +91-22-22782606, Fax number: +91-22-22804610

Figure S1

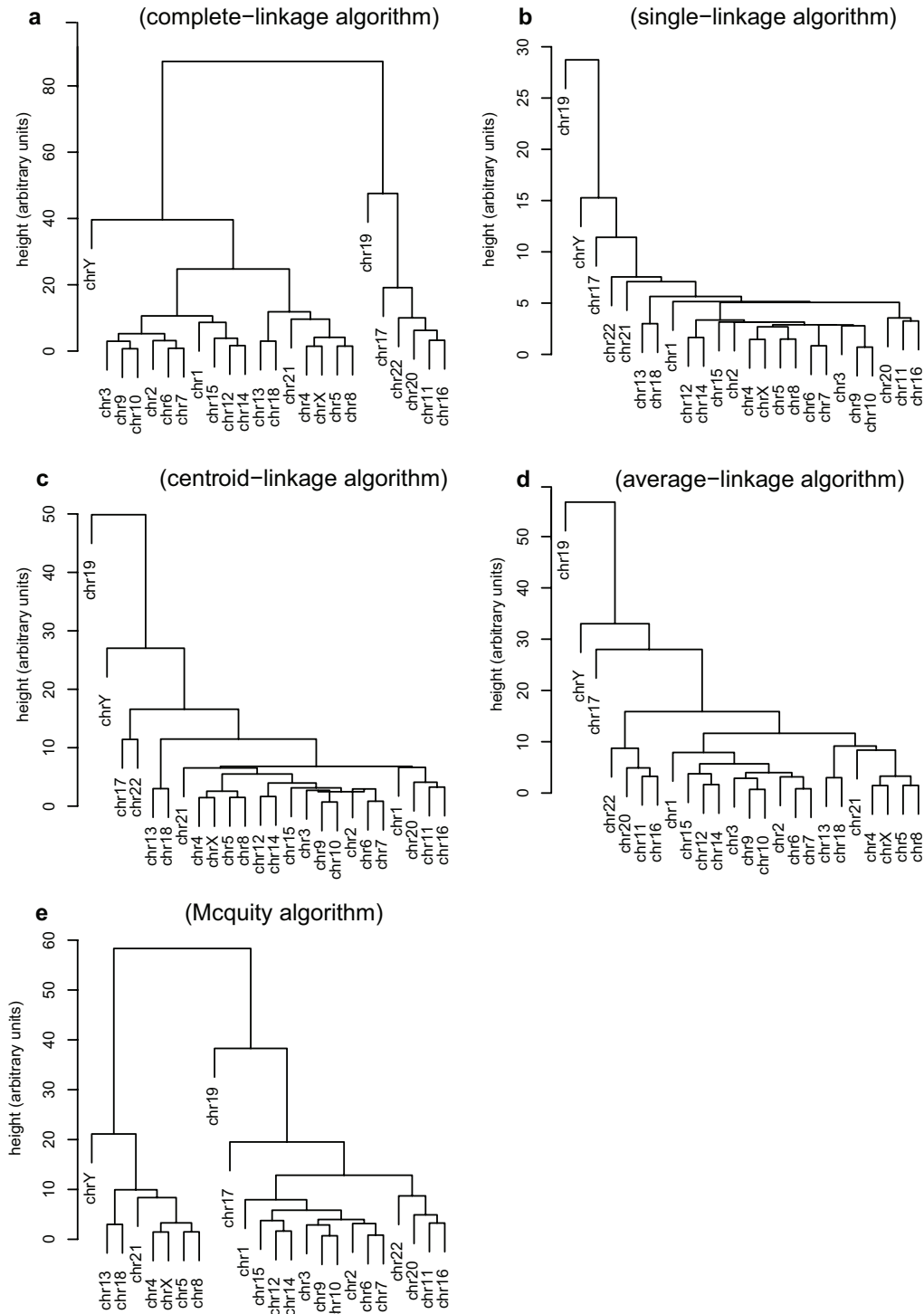


Figure S1. Hierarchical clustering of extrinsic effective gene density matrix computed using different algorithms. Dendrograms reveal the primary hierarchy of HSA19 (chr19), as obtained for CT pairs using the systems-level paired chromosome's gene count model, using five algorithms: complete-linkage (a), single-linkage (b), centroid-linkage (c), average-linkage (d), and Mcquity method (e).

Figure S2

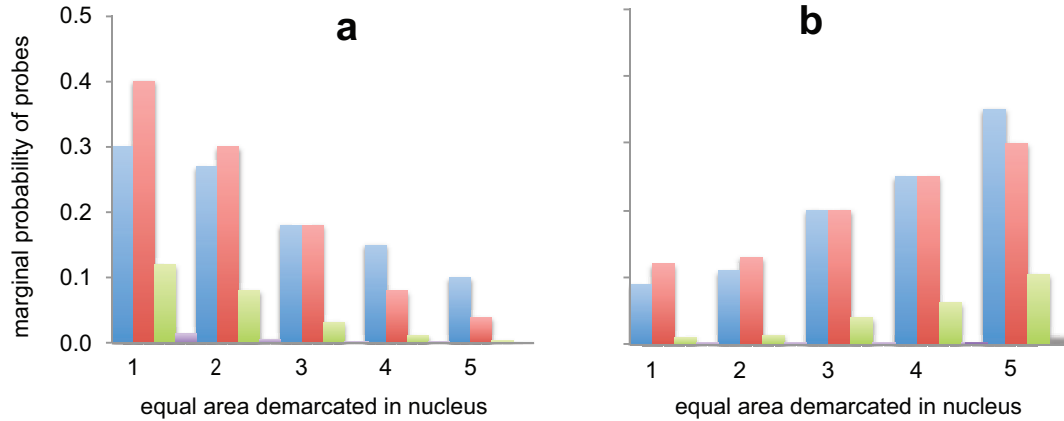


Figure S2. Bar graphs representing the spatial position of selected CTs in human interphase fibroblast nuclei. Marginal probability for aggregates of CTs in the nuclear spatial volume, which has been projected on to equal area annular 2D surface, is revealed as shells 1 – 5; shell 1 being toward the nuclear periphery and shell 5 at the nuclear interior. **(a)** Describes the probability distribution of probes from solo CTs chr18 (blue) and chr5 (red), the marginal probability of jointly finding one chr18 and one chr5 (green) (two chromosomes) and the marginal probability of jointly finding both homologs of chr18 and chr5 (violet) (four chromosomes). **(b)** Describes the probability distribution of probes from two “gene-rich” CTs, chr19 (blue) and chr17 (red), the marginal probability of jointly finding one chr19 and one chr17 (green) and the marginal probability of jointly finding both homologs of chr19 and chr17 (violet). The probability of finding individual probes was obtained from Mehta *et al.*, 2013.

Table S1. Preferential location of CTs obtained from normal human fibroblast and lymphocyte nuclei. A summary of dominant CT positions obtained from a population of human dermal fibroblast and lymphocyte nuclei using independent experimental microscopy studies. Experimental results from microscopy data were obtained for lymphocytes from Figure 3 as in ¹Boyle, *et al.* 2001, and for fibroblasts from Additional file 1 as in ⁸Mehta, *et al.* 2013. This table is a summary of those results. A 2D projection of FISH image from a nucleus was compartmentalized into five equal area annular shells, and maximal signal from the probed CT was ascribed to one of those annular shells: 1- 5 (Shells 1-2 were designated as peripheral, shell 3 as intermediate, and shells 4-5 as interior, see Fig. S2). FISH images from a clonal population of cells yields a distribution for CT position across these shells (Fig. S2). The most probable position for that CT will correspond to the shell where its distribution peaks. Here we compare peak distributions from lymphocytes and fibroblasts, for chr1-22, X and Y, from Boyle, *et al.* 2001 and Mehta, *et al.* 2013.

Chr ID	Lymphocyte nuclei ¹	Fibroblast nuclei ⁸	Summary
chr1	Interior – Intermediate	Intermediate – periphery	Inconsistent
chr2	Periphery	Periphery	Consistent
chr3	Periphery	Periphery	Consistent
chr4	Periphery	Periphery	Consistent
chr5	Intermediate	Periphery	Inconsistent
chr6	Interior –Intermediate – Periphery	Periphery	Inconsistent
chr7	Periphery	Periphery	Consistent
chr8	Periphery	Interior – Intermediate – Periphery	Inconsistent
chr9	Periphery	Periphery	Consistent
chr10	Intermediate	Interior – Intermediate – Periphery	<i>Weakly consistent</i>
chr11	Intermediate – Periphery	Periphery	<i>Weakly consistent</i>
chr12	Periphery	Periphery	Consistent
chr13	Periphery	Periphery	Consistent
chr14	Interior – Intermediate – Periphery	Interior – Intermediate – Periphery	Consistent
chr15	Intermediate	Periphery	Inconsistent
chr16	Interior – Intermediate	Intermediate – Periphery	Inconsistent
chr17	Interior	Interior	Consistent
chr18	Periphery	Periphery	Consistent
chr19	Interior	Interior	Consistent
chr20	Periphery	Interior - intermediate	Inconsistent
chr21	Interior – intermediate – Periphery	Interior	Inconsistent
chr22	Interior	Interior	Consistent
chrX	Periphery	Periphery	Consistent
chrY	Periphery	Interior	Inconsistent

Table S2. Corroboration of theoretical results with those obtained from independent Hi-C experiments. Corroboration of predicted inner core human CTs (Group A in our PCGC analysis) using results from two independent high-throughput studies. Column 2 represents the Group ID of individual CTs as obtained from our paired chromosome gene count study (Fig. 1a and Fig. 3). In column 3, the validity of our results of CT clustering is reported with respect to results in Figure 2B from Lieberman-Aiden *et al.* 2009. In column 4, our PCGC results of CT clustering (Group A) was validated with inner core Cluster 1 CTs in Figure 6C from Kalhor *et al.* 2012. Similarly, the Group B CTs were validated with respect to Cluster 2 from the same reference.

chrID	Hierarchy Group ID	Hi-C corroboration	TCC corroboration
chr1	B	Valid	Invalid
chr2	B	Valid	Valid
chr3	B	Valid	Valid
chr4	B	Valid	Valid
chr5	B	Valid	Valid
chr6	B	Valid	Valid
chr7	B	Valid	Valid
chr8	B	Valid	Valid
chr9	B	Insignificant	Valid
chr10	B	Valid	Valid
chr11	A	Invalid	Valid
chr12	B	Valid	Valid
chr13	B	Valid	Valid
chr14	B	Insignificant	Invalid
chr15	B	Insignificant	Invalid
chr16	A	Valid	Valid
chr17	A	Valid	Valid
chr18	B	Valid	Valid
chr19	A	Valid	Valid
chr20	A	Valid	Valid
chr21	B	Invalid	Invalid
chr22	A	Valid	Valid
chrX	B	Valid	Valid
chrY	B	Not available	Not available

Table S3. Results from sensitivity studies using intrinsic chromosomal parameters. The limiting values of gene reduction per chromosome that leads to an altered dendrogram computed using effective gene density.

chr ID	Minimum gene reduction for dendrogram change		Aprox % altered genome
	<i>Num. genes</i> (per chr)	<i>% genes</i> (per chr)	
chr1	300-400	8%-9%	1.0%
chr2	< 40	< 1%	0.1%
chr3	30-60	1%-2%	0.1%
chr4	70-100	4%-5%	0.2%
chr5	70-80	2%-3%	0.2%
chr6	200-250	7%-8%	0.5%
chr7	100-110	4%-5%	0.2%
chr8	70-100	3%-4%	0.2%
chr9	100-120	5%-6%	0.2%
chr10	70-80	3%-4%	0.2%
chr11	180-230	3%-4%	0.5%
chr12	80-90	2%-3%	0.2%
chr13	140-150	11%-12%	0.3%
chr14	40-50	1%-2%	0.1%
chr15	30-50	2%-3%	0.1%
chr16	10-20	<1%	0.1%
chr17	50-80	2%-3%	0.1%
chr18	40-50	5%-6%	0.1%
chr19	70-100	3%-4%	0.2%
chr20	20-30	2%-3%	0.1%
chr21	40-50	5%-6%	0.1%
chr22	40-50	4%-5%	0.1%
chrX	100-110	5%-6%	0.2%
chrY	50-60	10%-11%	0.1%

Table S4. Intrinsic parameters of chromosomes in the human genome. Intrinsic chromosomal parameters were obtained from NCBI's Gene and Mapviewer database.

chr ID	Number of genes per chr (n_j)	Chromosome length (L_j) (in Mbp)
chr1	4763	250
chr2	3598	242
chr3	2780	198
chr4	2251	190
chr5	2392	182
chr6	2825	171
chr7	2596	159
chr8	2003	145
chr9	2132	138
chr10	2040	134
chr11	2804	135
chr12	2396	133
chr13	1326	114
chr14	1949	107
chr15	1719	102
chr16	1842	90
chr17	2326	83
chr18	938	80
chr19	2420	59
chr20	1243	64
chr21	725	47
chr22	1129	51
chrX	1972	156
chrY	496	57